Electromechanical and Microwave S-Parameter Properties of a Wide Tuning Range MEMS Tunable Capacitor

Jinghong Chen, Jun Zou, Chang Liu, and Sung-Mo Kang
Department of Electrical & Computer Engineering, University of Illinois, Urbana, IL 61801

ABSTRACT

We present the electromechanical and microwave properties of a novel micromachined parallel-plate tunable capacitor with a wide tuning range. Different from conventional two-parallel-plate tunable capacitors, this novel tunable capacitor consists of one suspended top plate and two fixed bottom plates. One of the two fixed plates and the top plate form a variable capacitor, whereas the other fixed plate and the top plate are used to provide electrostatic actuation for capacitance tuning. For the fabricated prototype tunable capacitors, a maximum tuning range of 69.8% has been achieved experimentally, exceeding the theoretical tuning range limit (50%) of conventional two-parallel-plate tunable capacitors. This novel tunable capacitor also exhibits very low return loss (< 0.6dB between 45 MHz and 10GHz).

Keywords: tunable capacitor, simulation, S-parameter, dynamic.

INTRODUCTION

In recent years, MEMS technology has begun to be used in wireless communication systems to improve performance of existing devices based on structures or operational principles. RF components such as voltage-controlled oscillators (VCO) and tunable filters have been developed using MEMS technology. Young, *et al* reported a VCO [1] that contains a micromachined three-dimensional coil inductor [2] and a two-parallel-plate tunable capacitor with a tuning range of 16% [3]. Both passive elements are micromachined on silicon substrates and thus can be integrated with active circuit components using modified IC fabrication processes. In the past few years, as an important tunable RF component, tunable capacitors based on MEMS technology are under active development [4-7]. Compared with p-n junction varactors, MEMS tunable capacitors have the advantages of lower loss and potentially larger tuning range.

Among all the MEMS tunable capacitors developed to date, parallel-plate configuration (using electrostatic actuation) is the most commonly used. A parallel-plate tunable capacitor can be fabricated easily using surface micromachining techniques. However, the theoretical tuning range of such capacitors is limited to 50% by the *pull-in* effect. The actual achieved tuning range is often much smaller than the theoretical value due to parasitic capacitance (e.g. a measured tuning range of 16% was reported in [3]). Various broadband communication applications require a wide tuning range. Recently, much effort has been made to improve the tuning capability of MEMS tunable capacitors. Dec, *et al* [4] uses three-parallel-plate configuration (two suspended plates and one fixed plate on the substrate) to compensate the *pull-in* effect and obtain a tuning range of 87%. The fabrication process requires two layers of structural materials and two layers of sacrificial materials. Yao, *et al* [5] reported a tunable capacitor with a tuning range of 200%. It is based on lateral comb structures (instead of parallel plate) etched by deep reactive ion etching (DRIE) on SOI (silicon-on-insulator) substrate. Feng, *et al* [6] used a thermal actuator in their tunable capacitor and achieved a tuning range of 270%. The disadvantage of thermal actuators is that their response speed is generally slower than that of electrostatic actuators.

We report the development and modeling of a novel electrostatically actuated tunable capacitor. This new design keeps the simplicity of the conventional two-parallel-plate configuration, while providing a much wider tuning range. Only one structural layer and one sacrificial layer are used. The measured tuning range achieved was 69.8%, exceeding the 50% tuning range limit on conventional two-parallel-plate tunable capacitors. The capacitor operates under a wide frequency range (45 MHz to 10GHz) with signal loss below 0.6 dB. The new tunable capacitor is fabricated using standard surface micromachining process and thus can be monolithically integrated with IC circuits.

PRINCIPLE OF OPERATION

Fig. 1 shows a conventional parallel-plate tunable capacitor which consists of a suspended top plate and a fixed bottom plate, with an overlap area of A and initial spacing of x_0. When a DC voltage is applied across the two plates, the spacing between these two plates is reduced to x_0-x.

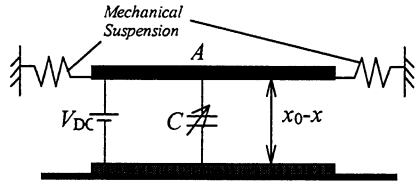

Figure 1: A schematic model of a conventional two-parallel-plate tunable capacitor with electrostatic actuation

Neglecting the fringe effect, the value of the capacitance between these two plates can be determined by

$$C = \frac{\varepsilon A}{(x_0 - x)} \tag{1}$$

When V_{DC} is applied, an attractive electrostatic force (F_e) is generated between the two plates with the value of F_e being

$$F_e = \frac{1}{2}\frac{\partial C}{\partial x}V_{DC}^2 = \frac{1}{2}\frac{CV_{DC}^2}{(x_0 - x)} \tag{2}$$

An effective spring constant k_e for the electrostatic force can be defined as

$$k_e = \left|\frac{\partial F_e}{\partial x}\right| = \frac{CV_{DC}^2}{(x_0 - x)^2} \quad (3)$$

The mechanical suspension of the top plate has a spring constant k_m. When the top plate is displaced, the suspension produces a restoring force, designated as F_m. The magnitude of F_m is related to x by $F_m = k_m x$. At equilibrium, the magnitudes of F_e and F_m are equal, thus

$$k_m x = \frac{CV_{DC}^2}{2(x_0 - x)} = \frac{1}{2} k_e (x_0 - x) \quad (4)$$

The expression of k_e in terms of k_m is

$$k_e = \frac{2k_m x}{(x_0 - x)} \quad (5)$$

Note that the two force constants are equal in magnitude when the value of x reaches $x_0/3$. The corresponding value of V_{DC} (at $x=x_0/3$) is called the *pull-in* voltage (V_{PI}). If V_{DC} is continuously increased beyond V_{PI} and x is beyond the critical point of $x_0/3$, no equilibrium position can be reached until the two plates are snapped into contact (*pull-in* effect). Thus the capacitance of the conventional two-parallel-plate tunable capacitor can only be controllably changed to 150% of its original value at most. Theoretically, the maximum controllable tuning range is then 50%.

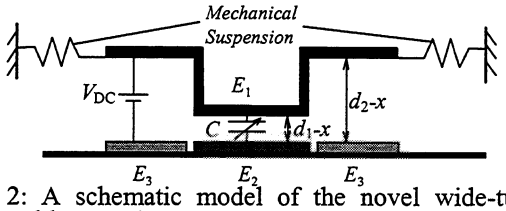

Figure 2: A schematic model of the novel wide-tuning-range tunable capacitor.

The schematic model of our novel wide-tuning-range tunable capacitor is shown in Fig. 2. It consists of three plates that are designated as E_1, E_2, and E_3. The plate E_1 is a movable top plate suspended by four cantilever beams. The plate E_2, which is fixed on the bottom substrate, forms a variable capacitor by coupling with the plate E_1. The plate E_3 (the outer fixed bottom plate) and E_1 are used to provide the electrostatic actuation. An actuation voltage (V_{DC}) is applied between plates E_3 and E_1. At rest (V_{DC}=0V), d_1 is designed to be smaller than d_2. When the plate E_1 (top movable plate) is moved by a distance of x under a given applied V_{DC}, the relative tuning range is derived as

$$\frac{C - C_0}{C_0} = \frac{\varepsilon A/(d_1 - x) - \varepsilon A/d_1}{\varepsilon A/d_1} = \frac{x}{d_1 - x} \quad (6)$$

This derived tuning range is valid as long as the pull-in effect between plates E_3 and E_1 does not occur, i.e. $x<d_2/3$. The values of d_1 and d_2 can be controlled by fabrication parameters. If $d_1 > d_2/3$, then the maximum tuning range can be found by plugging in $x=d_2/3$ into Eq. (6) which results in the maximum tuning range to be $d_2/(3d_1 - d_2)$. Since d_1 is smaller than d_2, the tuning range can be larger than 50%. In the case that $d_1 \le d_2/3$, the pull-in effect will not occur at all. Assuming the plates E_1 and E_2 can be pulled in to infinitely close distance, then theoretically, arbitrary tuning range can be achieved controllably. In reality, the achievable tuning range value also depends on other factors, such as surface roughness and curvature of E_2 and E_1.

FABRICATION

Surface micromachining technique is used to fabricate the prototype devices with Pyrex® glass wafer (1 mm thick) as the substrate. A unique process to realize the variable-height sacrificial layer (corresponding to d_1=2μm and d_2=3μm in Fig. 2) is developed. Thermally evaporated gold thin film is used as the material of the two fixed bottom plates E_2 and E_3, whereas the suspended top plate E_1 is made of electroplated Permalloy (nickel-iron alloy). Copper is used as the sacrificial layer material. Copper can be deposited using thermal evaporation and etched by a copper etchant ($HAC:H_2O_2:H_2O$=1:1:10), which has a very high etching selectivity between copper and the structure materials (Permalloy and gold). The copper layer can also serve as a seed layer for Permalloy electroplating.

The fabrication process is illustrated in Fig. 3. First, a 0.5-μm-thick gold film is thermally evaporated and patterned to make the two fixed plates E_2 & E_3 and contact pads for the suspended top plate E_1. Second, a 1-μm-thick copper film is thermally evaporated and patterned. Third, another 2-μm-thick copper film is thermally evaporated to form a variable-height sacrificial layer and a 2-μm-thick Ni-Fe alloy is deposited by electroplating using the copper as the seed layer. At last, the copper sacrificial layer is then etched and the entire device is released in a supercritical carbon dioxide (CO_2) dryer. Microscopic pictures of the fabricated prototype devices are shown in Fig. 4.

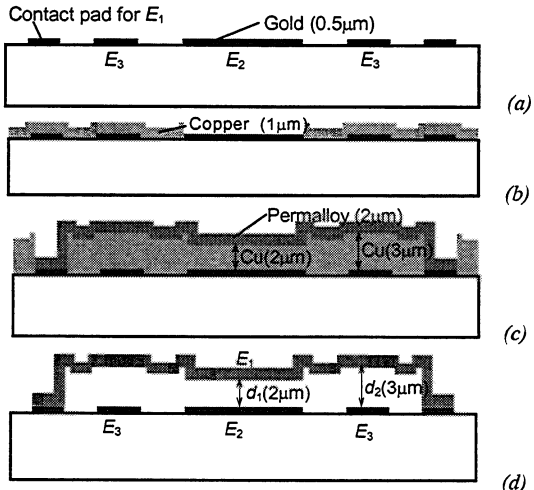

Figure 3: A schematic illustration of the fabrication process for the wide-tuning-range tunable capacitor.

In the fabricated prototype devices, the values of d_1, d_2 are 2μm and 3μm, respectively. In this case, d_1 can be tuned to 1μm ($d_2/3$) before the *pull-in* effect occurs between E_1 and E_3, which results in a maximum theoretical tuning range of 100% for the variable capacitance between E_1 and E_2.

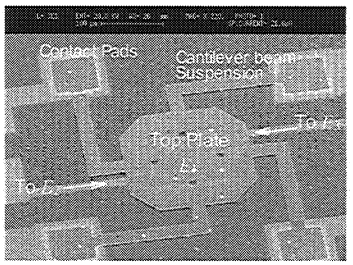

Figure 4: Microscopic pictures of the novel wide-tuning-range tunable capacitor

MODELING AND SIMULATION

The static electromechanical characteristic of tunable capacitor is simulated using the MEMCAD® 4.5 software. The calculated deformation of the suspended top plate caused by the electrostatic force (when V_{DC} = 18V) is shown in Fig. 5. The suspended top plate (E_1) remains flat and parallel to E_2 after the deformation. The simulated capacitance-voltage (C-V_{DC}) curve is plotted in Fig. 8 together with the measurement data, which shows a maximum tuning range of 90.8%. This is different from aforementioned theoretical value (100%) due to the account of fringe capacitance. The calculated change of d_1 as a function of V_{DC} is plotted in Fig. 7(b) together with the measurement data. When V_{DC} is greater than 19V, d_1 changes directly from 1 μm to zero, which means the *pull-in* voltage is about 19V from this simulation.

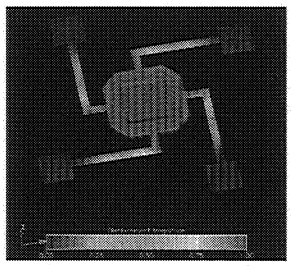

Figure 5: A 3D plot of the deformed suspended top plate E_1 when V_{DC} =18V.

The electromechanical dynamic behavior of the tunable capacitor is mathematically described by a second-order system that is dominated by spring force, inertia, and viscous damping as

$$m\frac{d^2x}{dt^2} + F_D + F_M = F_E \qquad (7)$$

where m is the mass of the top plate, F_D is the damping force, F_M is the spring force, and F_E is the electrostatic force. Static simulation combined with curve fitting is used to determine the different forces in Eq. (7). To determine F_E, the MEMCAD software is used to obtain the capacitance verses the top plate displacement (static simulation) for a set of V_{DC} inputs. A third-order polynomial is then used to fit the capacitance data as a function of the top plate displacement x. Such a derived $C(x)$ includes the fringing capacitance effect and thus can be more accurate than Eq. (1). The electrostatic force F_E is then determined as the spatial derivative of the electrostatic co-energy by using Eq. (2). Similarly, the spring force F_M verses the top plate displacement is determined by using MEMCAD static finite-element solver Abaqus for a set of mechanical loads, and is fitted using another third-order polynomial. The damping force is lumped approximated by using an experimental determined damping coefficient of 1.0×10^{-5} Ns/m in the simulation. The transient behavior of the tunable capacitor is then obtained by numerically solution of Eq. (7). Fig. 6 shows the dynamical behavior of the tunable capacitor device subject to a step input of V_{DC}=10V.

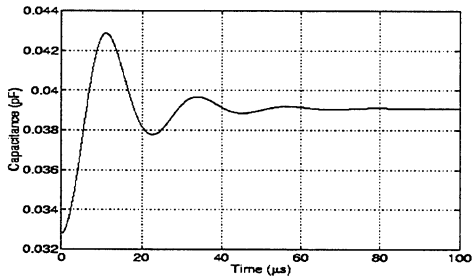

Figure 6: The dynamic response of the wide-tuning-range tunable capacitor subject to a step input of 10V.

The high frequency behavior of the wide-tuning-range tunable capacitor is simulated using Sonnet *em* Suite® software. The simulated S_{11} parameter when V_{DC} = 0V is plotted with the measurement data in Fig. 9.

Applied Voltage (V)	Displacement (μm)	Capacitance (pF)
1	0.03309274	0.032581
2	0.01151336	0.032977
3	0.02517205	0.033192
4	0.04428451	0.033498
5	0.06885116	0.033904
6	0.09887209	0.034409
7	0.1343474	0.035192
8	0.1752771	0.035768
9	0.2216611	0.036649
10	0.2734993	0.037688
11	0.3307913	0.038911
12	0.3935367	0.040367
13	0.4617347	0.042061
14	0.5353832	0.044066
15	0.6144817	0.046453
16	0.6990277	0.049321
17	0.7890187	0.052807
18	0.8844514	0.057161
19	0.985322	0.062577

Table-1: Static simulation of capacitance verse top plate displacement

TESTING AND MEASUREMENT

The surface profile of the tunable capacitor at different values of V_{DC} is measured using the WYKO® NT1000 optical surface profiler. Fig. 7 (a) show the measured surface profile plotted in 3-D graphs when V_{DC}=16V. The change of the spacing d_1 as a function of V_{DC} is extracted from the surface profile measurement (Fig. 7(b)). When V_{DC} increases from 0V to 20V, d_1 decreases continuously from 2 μm to 1.2 μm until

the *pull-in* effect occurs at V_{DC}=17.2V. When V_{DC} decreases from 20V to 0V, the suspended top plate E_1 is observed not to recover from the *pull-in* effect until V_{DC} drops to 15.8V. When the *pull-in* effect occurs, the suspended top plate E_1 does not completely contact with the fixed plate E_2 since d_1 cannot be decreased to 0. Possible reasons are surface roughness of the two plates E_1 and E_2, the existence of residual film from sacrificial layer etching, or absolute measurement calibration.

Five identical prototype devices fabricated on one substrate are tested using HP 4284A precision LCR meter at the frequency of 1 MHz (Fig. 8). The *pull-in* effect is observed at a DC bias of approximately 17-20 volts. The difference in the *pull-in* voltage among the five tested devices is due to the difference in the stiffness of the four-cantilever beam suspension, resulting from the thickness variance from 1.71μm to 1.84μm. The maximum tuning ranges of the five devices are 50.9%, 44.7%, 55.6%, 59.2%, and 69.8%. The parasitic capacitance associated with each device in the measurement setup is believed to cause the decrease in the achievable tuning range.

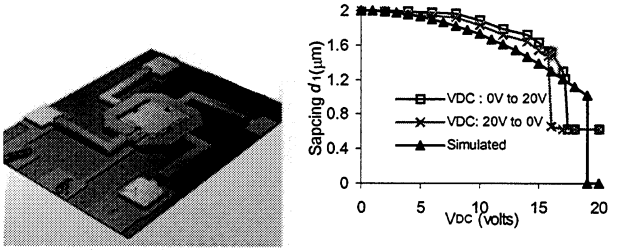

Figure7: (a) 3-dimensional plots of the measured surface profile of the novel wide-tuning-range tunable capacitor by WYKO®NT1000 optical profiler: V_{DC}=16V. (b) The measured vs. simulated d_1 as a function of V_{DC}.

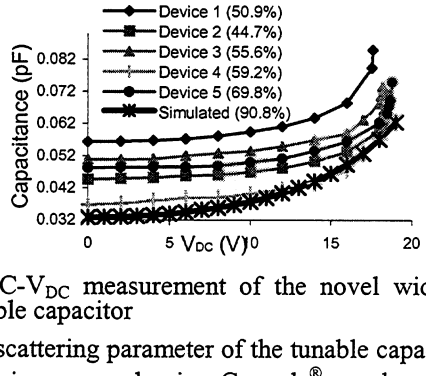

Figure 8: C-V_{DC} measurement of the novel wide-tuning-range tunable capacitor

The S_{11} scattering parameter of the tunable capacitor (when V_{DC} = 0V) is measured using Cascade® co-planar GSG-150 probe and HP 8510B network analyzer from 45 MHz to 10 GHz. The measurement result is plotted in Fig. 9, which shows a nearly ideal capacitive behavior in the tested frequency range with a return loss lower than 0.6dB. The measurement data closely matches the simulation data.

CONCLUSION REMARKS

We have presented the development and modeling of a novel electrostatically actuated wide-tuning-range MEMS tunable capacitor. Electromechanical (both static and dynamic) and microwave S-parameter simulations are performed. Due to the small but finite intrinsic stress of the Permalloy film, the size of the suspended top plate E_1 is made smaller than 500μm×500μm. This limits the base capacitance of the tunable capacitor. The development of a parallel tunable capacitor array to increase the overall capacitance value (Fig. 10) is underway.

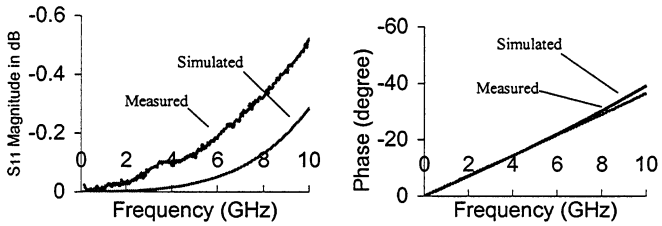

(a) (b)

Figure 9: The simulated vs. measured S_{11} parameter of the tunable capacitor: (a) magnitude, (b) phase.

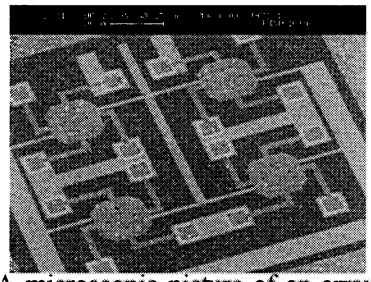

Figure 10: A microscopic picture of an array of 4 wide-tuning-range tunable capacitors.

REFERENCES

1. D. Young, V. Malba, J. Ou, A. Bernhardt, B. Boser, "A low-noise RF voltage-controlled oscillator using on-chip high-Q three dimensional coil inductor and micromachined variable capacitor", *Tech. Digest of Solid-state sensors and actuator workshop*, Hilton Head Island, SC, pp. 128-131, 1998.
2. D. Young, V. Malba, J. Ou, A. Bernhardt, and B. Boser, "Monolithic high-performance three-dimensional coil inductors for wireless communication applications", *IEDM Dig. Tech. Papers*, pp. 67-70, 1997.
3. D.J. Young and B.E. Boser, "A micromachined variable capacitor for monolithic low-noise VCOs", *Tech. Digest of Solid-state sensors and actuator workshop*, Hilton Head Island, SC, pp. 86-89, 1996.
4. A. Dec and K. Suyama, "Micromachined varactors with wide tuning range," *IEEE transactions on microwave theory and techniques*, Vol. 46, No. 12, pp. 2587-96, 1998.
5. J. Yao, S. Park and J. DeNatale, "High tuning ratio MEMS based tunable capacitors for RF communications applications," *Tech. Digest, solid-state sensors and actuators workshop*, Hilton Head Island, SC, pp. 124-127, 1998.
6. Z. Feng, H. Zhang, W. Zhang, B. Su, K. Gupta, V. Bright, Y. Lee, "MEMS-based variable capacitor for millimeter-wave applications" *Tech. Digest, solid-state sensors and actuators workshop*, Hilton Head Island, SC, pp. 255-258, 2000.
7. S.M. Kang and J.H. Chen, "Computer Aided Design for Mixed-Technology VLSI Systems", accepted by *IEEE Asian Pacific Conference on Circuits and Systems*, Tianjin, China, December, 2000